Appl. Chem. Eng., Vol. 31, No. 6, December 2020, 697-700
https://doi.org/10.14478/ace.2020.1092

Communication

석영 나노 결정의 합성과 특성

문규섭 · 정성욱*,†

부산대학교 화학공학 · 고분자공학과, *부산대학교 응용화학공학부
(2020년 11월 10일 접수, 2020년 11월 16일 수정, 2020년 11월 21일 채택)

Synthesis and Characterization of Quartz Nanocrystals

Gyuseop Moon and Sungwook Chung*,†

Department of Polymer Science and Chemical Engineering, Pusan National University, Busan 46241, Republic of Korea
**School of Chemical and Biomolecular Engineering, Pusan National University, Busan 46241, Republic of Korea*
(Received November 10, 2020; Revised November 16, 2020; Accepted November 21, 2020)

초 록

본 연구에서는 석영 나노 결정의 합성과 특성 분석을 진행하였다. 비정질 실리카 나노 입자 전구체가 용해된 용액을 섭씨 250도 온도와 자가 압력의 온건한 열수 반응 하에서 석영 나노 결정을 성공적으로 합성하였다. 합성된 나노 결정의 화학적 조성과 구조 분석을 시행하였다. 알파 석영의 특징적인 고결정질 상의 나노 구조를 가지는 석영 나노 결정의 평균 크기는 반응 시간에 따라 407.5 에서 826.2 nm까지 비교적 좁은 범위에서 조정될 수 있음을 발견하였다. 본 연구를 통해 발견된 석영 나노 입자는 광전자, 센서, 및 충전식 배터리 소자의 기술 응용에 매우 중요한 잠재적 용도가 있을 것으로 사료된다.

Abstract

We report the synthesis and characterization of quartz nanocrystals (NCs). Quartz NCs were synthesized from the dissolution of amorphous silica nanoparticle precursors under the mild hydrothermal condition of ~250 ℃ and autogenic pressure. It was confirmed that the average size of the nanostructure with a highly crystalline phase of α-quartz can be tuned in a relatively narrow range from 407.5 to 826.2 nm with respect to the reaction time. α-Quartz NCs have potential uses for technological applications in optoelectronics, sensing, and rechargeable battery devices.

***Keywords**: Silicon dioxide, Quartz, Nanocrystals, Nanoparticles, Hydrothermal reaction*

1. Introduction

Silica is one of the most fundamental mineral components found in the Earth's soil. There are a number of different uses of silica as industrial and engineering materials to make products for improving our quality of life. One of the commonly occurring forms of crystalline silica is quartz because it is the most thermodynamically stable phase under ambient conditions. Quartz is a chemically inert and relatively hard crystalline mineral present in soils and rocks. It has two polymorphs of α- and β-quartz that have slightly different crystal symmetries[1]. In general, only α-phase is stable at ambient temperature and atmospheric pressure[2].

Hydrothermal growth of quartz crystals has been studied extensively for more than almost fifty years[3,4]. A few examples of synthesizing quartz nanocrystals (NCs) with sizes from hundreds of micrometers to tens of nanometers have been demonstrated via hydrothermal routes [5-8]. Unfortunately, the reported methods did not always guarantee excellent control over well-defined sizes, shapes, and crystal phases likely due to extremely fast nucleation and growth rates and rapid coarsening under highly alkaline hydrothermal conditions[5,7]. In this communication, we report an improved hydrothermal method to synthesize quartz NCs from precursors of amorphous silica nanoparticles (ASNs) dissolved in aqueous solutions. We show that as-synthesized NCs have a highly crystalline phase of α-quartz and have relatively uniform sizes ranging from 407.5 to 826.2 nm that predominantly depend on their reaction time from 6 to 24 h.

2. Materials and Methods

Quartz NCs were synthesized via a hydrothermal reaction based on

† Corresponding Author: Pusan National University,
School of Chemical and Biomolecular Engineering, Busan 46241, Republic of Korea
Tel: +82-51-510-2397 e-mail: sungwook.chung@pusan.ac.kr

pISSN: 1225-0112 eISSN: 2288-4505

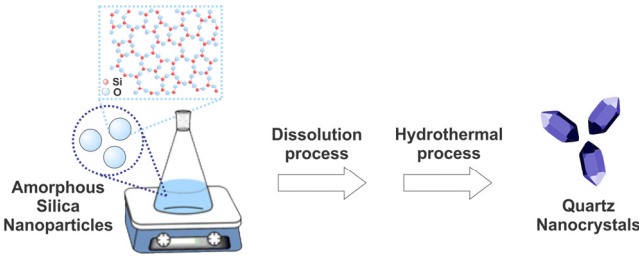

Figure 1. Schematic illustration of the preparation of quartz nanocrystals (NCs) from amorphous silica nanoparticles (ASNs) via a hydrothermal method (For interpretation of the references to color in this figure legend, the reader is referred to the web version of this communication).

the scheme shown in Figure 1. An aqueous solution of 0.225 g ASNs prepared via a slightly modified Stöber process[8-10] mixed with 27 mL triply distilled H_2O and 3 mL 1N sodium hydroxide (NaOH) solution was heated at 100 ℃ and stirred at 400 rpm for 1 h. The solution turned from murky white to clear after ~20 min likely due to the complete dissolution of ASNs at pH ~12. After 1 h, ~1 mL of 1N hydrochloric acid (HCl) was added to eliminate excess hydroxyl ions by partially neutralizing the solution at pH ~7.0. The resulting solution was transferred to a 50 mL polyether etherketone (PEEK)-lined stainless steel autoclave and heated to ~250 ℃ over the time period of 3~24 h. Once the reaction was complete, the autoclave was slowly cooled to room temperature. The white precipitates were then filtered through a Nylon membrane with a pore diameter of 0.25 μm, washed with an excess of deionized water and absolute ethanol and dried in a vacuum oven at room temperature to yield ~120 mg of the NCs.

X-ray powder diffraction (XRD) data of the NCs were recorded by using a Philips X'Pert-MPD Diffractometer (Philips Inc., USA) with a monochromatized source of Cu Kα1 radiation (λ = 0.15405 nm) at 1.2 kW power (40 kV, 30 mA). Fourier transform infrared spectroscopy (FT-IR) was performed by using a Spectrum GX FT-IR spectrometer (Perkin Elmer Inc., USA) with both KBr pellets and attenuated total reflection (ATR) techniques. X-ray photoelectron spectroscopy (XPS) data of the NCs were acquired using an ESCALAB 250 spectrometer (Thermo Fisher Scientific Inc., USA) with a monochromatic X-ray source of Al anode K$_\alpha$ radiation (1486.6 eV) as an excitation source. The binding energy was calibrated to the C 1s line of carbon at 284.6 eV before the actual measurements. The morphologies of the NCs were investigated by field emission scanning electron microscopy (FESEM) performed on Zeiss Supra 25 microscope (Zeiss International, Germany) with an accelerating voltage ranged from 5 to 10 kV. Transmission electron microscopy (TEM) of the NCs was performed on Hitachi H-7600 TEM (Hitachi High-tech, Germany) operated at an accelerating voltage of 80 kV. High-resolution TEM (HRTEM) and selected area electron diffraction (SAED) analysis were performed on a TALOS F200X TEM (FEI & Thermo Fisher Scientific Electron Microscopy Solutions, USA) at an acceleration voltage of 200 kV. ^{29}Si solid-state nuclear magnetic resonance (ssNMR) spectroscopy of the NCs and ASNs was performed on a 400MHz AVANCE III HD NMR spectrometer (Bruker Corporation) equipped with a 4 mm (outer diameter of

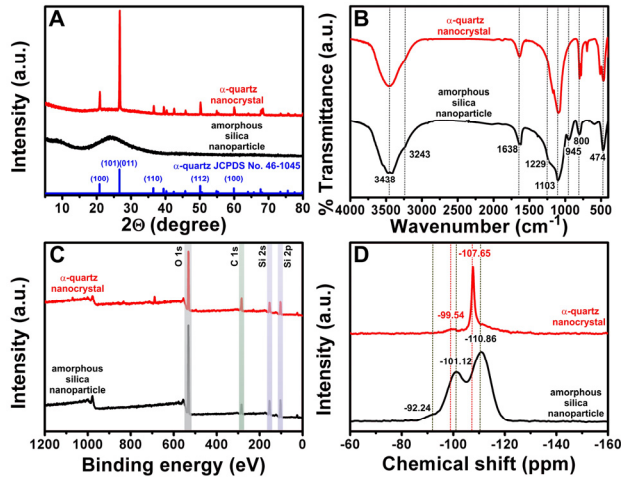

Figure 2. (A) XRD patterns, (B) FT-IR spectra, (C) XPS spectra, and (D) ^{29}Si ssNMR spectra of α-quartz NCs (red) and ASNs (black) (For interpretation of the references to color in this figure legend, the reader is referred to the web version of this communication).

zirconia rotor) magic angle spinning (MAS) probe at Korea Basic Science Institute (KBSI, Western Seoul Center, Korea). Spectra were obtained using direct excitation at 79.51 MHz with a 1.6 μs pulse width (pulse angle $\pi/6$), a 50 s recycle delay at ambient probe temperature (~25 ℃), and a sample spin rate of 11 kHz. Signals from 4900 scans were accumulated. ^{29}Si NMR chemical shifts (δ in ppm) were referenced versus an external sample of tetrakis(trimethylsilyl) silane at -135.5 ppm with respect to tetramethylsilane (TMS) at 0.0 ppm.

3. Results and Discussion

Figure 2 shows XRD, FT-IR, XPS, and ^{29}Si ssNMR measurements of α-quartz NCs. Figure 2A shows the XRD patterns of the as-synthesized NCs. All the peaks in the XRD pattern (red curve) were consistent with that of bulk α-quartz (blue curve, Joint Committee on Powder Diffraction Standards (JCPDS) card no. 46-1045). FT-IR spectrum of the as-synthesized α-quartz NCs (red curve, Figure 2B) exhibited IR absorption bands at 3438 and 3243 cm^{-1} and they were assigned to the hydroxy stretching vibration of adsorbed water and surface silanol[11]. The band at 1638 cm^{-1} was assigned to the bending vibration of adsorbed water[11]. IR bands at 1103, 800, and 474 cm^{-1} were attributed to asymmetric and symmetric stretching and symmetric bending of Si-O-Si functional moieties[12]. In general, the FT-IR spectrum obtained from α-quartz NCs was comparatively analogous to one from ASNs precursor except for the fingerprint region from 1000 to 400 cm^{-1} and a missing band at 945 cm^{-1}, which was likely due to fewer free hydroxy groups bound to the surface Si of α-quartz NCs. Survey XPS spectra of α-quartz NCs and ASNs (Figure 2C) likewise provided very similar binding energies (BEs) of Si 2p peaks at 103.1 eV and O 1s peak at 532.1 eV. However, the results of ^{29}Si ssNMR spectroscopy explicitly showed that they were dissimilar in the chemical environments of their silica networks. ^{29}Si ssNMR spectrum of ASNs (black curve, Figure 2D) showed three characteristic peaks at -92.24,

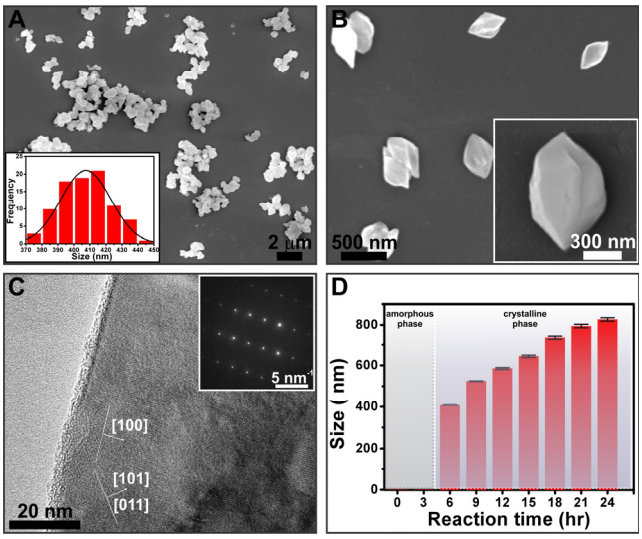

Figure 3. (A) Representative FESEM image of as-synthesized α-quartz NCs and their histogram of the measured sizes, (B) Higher magnification FESEM image of α-quartz NCs showing their unique oblong morphologies, (C) HRTEM image of single α-quartz NC exhibiting lattice fringes of the (100), (010), and (011) planes, and (D) Bar plot showing the measured reaction time dependence of the size of the NCs (For interpretation of the references to color in this figure legend, the reader is referred to the web version of this communication).

-101.12, and -110.86 ppm, which were assigned to dihydroxy terminated Q^2 [$(-O)_2Si(OH)_2$], monohydroxy terminated Q^3 [$(-O)_3Si(OH)$], and nonhydroxy terminated Q^4 [$(-O)_4Si$] sites, respectively. On the contrary, ^{29}Si ssNMR spectrum of α-quartz NCs (red curve, Figure 2D) rather showed a major Q^4 peak at -107.65 ppm with much narrower spectral width, which was likely due to both a predominant population of non-hydroxy terminated sites and less change in Si-O-Si angles in highly ordered silica networks of the crystalline NCs[8].

Figure 3 shows FESEM and HRTEM micrographs of the NCs. As-synthesized NCs displayed a similar shape and morphology of bulk quartz with an apparent crystal shape that has a six-sided prism with two six-sided pyramids at both ends (inset image of Figure 3B). Based on FESEM measurements of Figure 3A, the average size of the NCs synthesized from 6 h reaction time was measured to be 407 ± 16 nm with a slightly skewed distribution (inset histogram of Figure 3A). HRTEM micrograph of typical α-quartz NCs (Figure 3C) showed lattice fringes exhibiting highly crystalline domains of (101) and (011) planes separated from domains of (100) by grain boundary. Likewise, the degree of crystallinity was revealed by a set of ordered spots that were assigned to (100), (101), and (011) planes (inset image of Figure 3C), which was also confirmed by calculated *d*-spacings from independent measurements of SAED. These *d*-spacings of 0.426, 0.334, and 0.334 nm were in excellent agreement with the (100), (101), and (011) reflections of XRD patterns shown in Figure 2A, respectively.

Figure 3D shows the measured reaction time dependence of the length and width of the NCs. A few aspects of the growth process are worth addressing. First, immediately after the start of the hydrothermal reaction, the products formed over the period of 0~3 h appeared to have amorphous structures confirmed by XRD and ^{29}Si ssNMR measurements. Second, the results of XRD measurements revealed the emergence of the crystallinity of α-quartz after the induction period of ~3 h, implying that the structure and order of the silica network likely began to emerge in the products of the NCs. Third, their growth exhibited a power-law dependence on the reaction time *t* of the NC formation with the exponent α of the form At^{α} close to ~0.5. Currently, we do not fully understand the mechanism of the growth of the NCs. It is likely that the mechanism may follow classical principles of nucleation and growth of colloidal nanoparticles and nanocrystals. Further studies on the growth of the NCs are still ongoing and their in-depth analyses will shed light on the elucidation of the growth mechanism. The complete analyses of the growth kinetics will be reported in the near future.

4. Conclusions

We successfully synthesized α-quartz NCs from ASN precursor solutions under mild hydrothermal conditions of ~250 ℃ and autogenic pressure. The structure, morphology, and composition of the NCs were characterized using FT-IR, ssNMR, XPS, XRD, FESEM, and HRTEM measurements systematically. As-synthesized NCs exhibited highly crystalline nanostructures of α-quartz and their average size can be tuned in a relatively narrow range from 407.5 to 826.2 nm with reaction time. Additional studies of characterizing the processes' growth kinetics will be required to understand the mechanism responsible for the formation of quartz NCs in the near future. In summary, our results provide a facile means of producing quartz NCs of high crystal quality and relatively narrow size distributions, offering potential uses for technological applications in optoelectronics, sensing, and rechargeable battery devices.

Acknowledgements

This work was supported by a 2-Year Research Grant of Pusan National University.

References

1. C. H. Yoder, *Ionic Compounds: Applications of Chemistry to Mineralogy*, 1st ed., 173-175, John Wiley & Sons, NJ, USA (2006).
2. H. Grimm and B. Dorner, On the mechanism of the α-β phase transformation of quartz, *J. Phys. Chem. Solids*, **36**, 407-413 (1975).
3. P. Bettermann and F. Liebau, Transformation of amorphous silica to crystalline silica under hydrothermal conditions, *Contrib. Mineral Petrol.*, **53**, 25-36 (1975).
4. W. S. Fyfe and D. S. McKay, Hydroxyl ion catalysis of the crystallization of amorphous silica at 330 °C and some observations on the hydrolysis of albite solutions, *Am. Mineral.*, **47**, 83-89 (1962).
5. J. F. Bertone, J. Cizeron, R. K. Wahi, J. K. Bosworth, and V. L. Colvin, Hydrothermal synthesis of quartz nanocrystals, *Nano Lett.*, **3**, 655-659 (2003).
6. P. Buckley, N. Hargreaves, and S. Cooper, Nucleation of quartz under ambient conditions, *Commun. Chem.*, **1**, 49 (2018).

7. X. M. Jiang, Y. B. Jiang, and C. J. Brinker, Hydrothermal synthesis of monodisperse single-crystalline alpha-quartz nanospheres, *Chem. Commun.*, **47**, 7524-7526 (2011).
8. G. Moon, N. Lee, S. Kang, J. Park, Y.-E. Kim, S.-A. Lee, R. K. Chitumalla, J. Jang, Y. Choe, Y.-K. Oh, and S. Chung, Hydrothermal synthesis of novel two-dimensional α-quartz nanoplates and their applications in energy-saving, high-efficiency, microalgal biorefineries, *Chem. Eng. J.,* Doi:10.1016/j.cej.2020.127467.
9. E.-H. Jang, S. P. Pack, I. Kim, and S. Chung, A systematic study of hexavalent chromium adsorption and removal from aqueous environments using chemically functionalized amorphous and mesoporous silica nanoparticles, *Sci. Rep.*, **10**, 5558 (2020).
10. W. Stöber, A. Fink, and E. Bohn, Controlled growth of monodisperse silica spheres in the micron size range, *J. Colloid Interface Sci.*, **26**, 62-69 (1968).
11. M. Takeuchi, G. Martra, S. Coluccia, and M. Anpo, Evaluation of the adsorption states of H_2O on oxide surfaces by vibrational absorption: Near- and mid-infrared spectroscopy, *J. Near Infrared Spec.*, **17**, 373-384 (2009).
12. B.-G. Kim, S.-Y. Kang, and J.-J. Kim, FTIR study of fluorinated silicon oxide film, *J. Phys. D: Appl. Phys.*, **30**, 1720-1724 (1997).

Authors

Gyuseop Moon; Ph.D. Candidate, B.Sc., Department of Polymer Science and Chemical Engineering, Pusan National University, Busan 46241, Republic of Korea; jhmoon26@pusan.ac.kr

Sungwook Chung; Associate Professor, Ph.D., School of Chemical and Biomolecular Engineering, Pusan National University, Busan 46241, Republic of Korea; sungwook.chung@pusan.ac.kr